Supporting information: A simple RNA-DNA scaffold templates the assembly of monofunctional virus-like particles

Rees F. Garmann[1,4], Richard Sportsman[1], Christian Beren[1], Vinothan N. Manoharan[4,5], Charles M. Knobler[1], William M. Gelbart[1,2,3]

[1]Department of Chemistry and Biochemistry, [2]California NanoSystems Institute, and [3]Molecular Biology Institute, University of California, Los Angeles, Los Angeles, CA 90095, USA.
[4]Harvard John A. Paulson School of Engineering and Applied Sciences, and [5]Department of Physics, Harvard University, Cambridge, MA 02138, USA.

Synthesis of capsid protein

Capsid protein (CP) was purified from wild-type cowpea chlorotic mottle virus (CCMV) grown in California cowpea plants (*Vigna ungiculata* cv Black Eye) as described by Annamalai and Rao[1]. Briefly, virions were disrupted by 24-h dialysis against disassembly buffer (1M $CaCl_2$, 50 mM Tris pH 7.5, 1 mM EDTA, 1 mM DTT, and 0.5 mM PMSF) at 4°C. The RNA was pelleted by ultracentrifugation at 4×10^5 g for 90 min and the CP was extracted from the supernatant in separate fractions. Each fraction was immediately dialyzed against protein buffer (1M NaCl, 20 mM Tris pH = 7.2, 1 mM EDTA, 1 mM DTT, and 1 mM PMSF). The protein concentration and its purity, with respect to RNA contamination, were measured by UV-Vis spectrophotometry – only protein samples with 280/260 ratios greater than 1.5 (less than 5% RNA contamination) were used for assembly. SDS-PAGE gel electrophoresis and MALDI-TOF showed no evidence of cleaved protein.

Synthesis of RNA

Fluorecently labeled brome mosaic virus genomic RNA1 (B1) was synthesized by *in vitro* transcription of a linearized DNA template by T7 RNA polymerase and fluorescent rUTP-AF488 (ChromaTide® Alexa Fluor® 488-5-UTP; Molecular Probes, U.S.A.). A rATP:rGTP:rCTP:rUTP:rUTP-AF488 molar ratio of 600:600:600:5.32:1 was used and resulted in a density of labeling of 0.5 rUTP-AF488s per RNA. After transcription, the template DNA was digested by DNase I (New England Biolabs), and the resulting fragments removed by washing five times with a 20-fold excess of TE buffer (10mM Tris pH 7.5, 1 mM EDTA) using a 100-kDa MWCO centrifugal filter device (EMD Milipore) operated at 5,000 g.

Design and Synthesis of DNA

The DNA splint strand was purchased from Integrated DNA Technologies. The sequence is shown below:

5'-AATCTGCGCAGATAACTGTTGCGCGACCTGA
TTGTCTACGATGTCTTGGGCACTCTGGCTGGCA
GCACCCTTCTCAGCAATCAACTTCAGCAAATCG
ATAGAACTTGACATTTTGTTGGTGAAAAACAAAG
AACAAGTAGCAGAACCGTGGTCGACAAGGGAT
TGAACCTCGTTCCGTGGTCTACAAAAAAAAAAA
AAAA-3'

This sequence consists of the reverse complement of the first 185 bases of the 5' terminus of B1 RNA followed by poly-A_{15}.

We did not test whether DNA splints with complementary sequences shorter than 185 bases are capable of templating the assembly of cherry bombs, though we suspect this is the case. Assuming that the rise of hybridized ds-RNA-DNA is intermediate between those of ds-DNA (0.34 nm per bp) and ds-RNA (0.25nm per bp), the physical length of a 185 bp hybrid strand measures about 55 nm, 2-3 times the inner diameter (22 nm) of the CCMV capsid. Therefore, we expect that much shorter DNA splints (as short as, say, 80 bases) should lead to hybrid ds-RNA-DNA portions that are too long to be packaged. However, these cherry bombs would have "fuses" that extend a shorter distance from the

capsid. Alternatively, multiple short DNA splints designed to bind adjacent RNA sequences might be used to generate a more flexible fuse, due to the nicks between each pair of neighboring splints.

Fluorescent Poly-T$_{15}$ was similarly purchased with 6-FAM conjugated to the 5'-terminus.

Hybridization of the RNA-DNA scaffold

RNA-DNA hybridization was performed by mixing a 1:1 molar ratio of B1 RNA and splint DNA, each at 1µM, in hybridization buffer (10mM Tris pH 7.5, 200 mM NaCl, 1 mM EDTA), heating to 90°C for 1 min, cooling to 55°C for 3 min, and cooling to 4°C indefinitely.

Co-assembly of CCMV CP and the hybrid RNA-DNA scaffold – assembling the cherry bomb

Assembly was carried out as described in our earlier packaging studies involving CCMV CP and pure RNA[2–4]. Briefly, the RNA-DNA scaffold (final concentration 1nM) was mixed with purified CCMV CP in a ratio (wt/wt) of 6:1 in protein buffer and then dialyzed overnight at 4 °C against assembly buffer (50 mM NaCl, 10 mM KCl, 5 mM MgCl2, 1 mM DTT, 50 mM Tris-HCl pH 7.2). The samples were then dialyzed against virus suspension buffer (50 mM sodium acetate, 8 mM magnesium acetate pH 4.75) for at least 6 h to complete the assembly process. The products were then concentrated using a 100 kDa MWCO centrifugal filter device (EMD Milipore) operated at 3,000 g.

The yield of cherry bombs – the fraction of RNA-DNA hybrids that are packaged by protein into capsids, with the ssDNA end accessible outside – was difficult to quantify by direct visualization by TEM because of the faint signal from the exposed RNA-DNA fuse. The majority of the assembly products appeared as well-formed capsids, but the number of capsids with a clearly visible fuse (Fig. S1) was low. However, native agarose gel electrophoresis showed that equilibrating roughly equal molar concentrations of cherry bombs and fluorescently labeled poly-dT (Fig. 4) resulted in all of the poly-dT signal comigrating with the cherry bombs (see lane 3 of Fig. 4) – suggesting that most of the RNA-DNA hybrids were packaged and that the resulting cherry bombs had functional fuses.

Decorating 30-nm gold nanoparticles with short DNA strands

30-nm diameter gold nanoparticles (AuNPs) were functionalized following the protocol described by Hurst, Lytton-Jean, and Mirkin[5]. Briefly, 20 nmoles of

5' dithiol-terminated Poly-T$_{25}$ DNA oligos (Integrated DNA Technologies) were incubated with DTT (0.1M DTT, 0.18M phosphate buffer, pH 8) for 1 h at room temperature. The DTT was then removed with a Nap-5 column (Sephadex G-25 DNA Grade), and the purified oligo concentration was determined by UV-visible spectroscopy. 2 nmoles of deprotected, thiolated Poly-T$_{25}$ oligos (final concentration of 1 µM) were added to 1 ml of 30 nm citrate-stabilized gold nanoparticles (Nanopartz Inc., OD=1, 0.05 mg/ml, final concentration of 300 pM) and the mixture was brought to 0.01M phosphate buffer pH 7, 0.01% SDS. The reaction was mixed and sonicated thoroughly, then incubated on a rotator for 2 h in the dark. The conjugation mix was incrementally introduced to higher salt conditions in the following way: 12.5 µL of 2M NaCl was mixed thoroughly into the reaction vessel, followed by sonication and a 1 h incubation. This procedure was repeated a total of 6 times, bringing the final concentration of NaCl to 0.1M. After salting, the reaction mix was left on a rotator overnight in the dark. To remove unbound DNA oligos, the solution was centrifuged at 10,000 g for 20 minutes, the supernatant was removed, and the gold nanoparticle pellet was resuspended in 1 ml 0.01M phosphate buffer pH 8, 0.1M NaCl, 0.01% SDS. This was repeated 3 times, and the final pellet resuspended in 0.01M phosphate buffer pH 8, 0.1M NaCl. The products were imaged by negative-stain TEM (Fig. S2), which revealed a faint ring of material surrounding the electron-dense AuNP that most likely corresponds to the DNA coat. The number of Poly-T$_{25}$ oligos coating the nanoparticles was not quantified, but oligo-coating was tested qualitatively using a salt-stability assay.
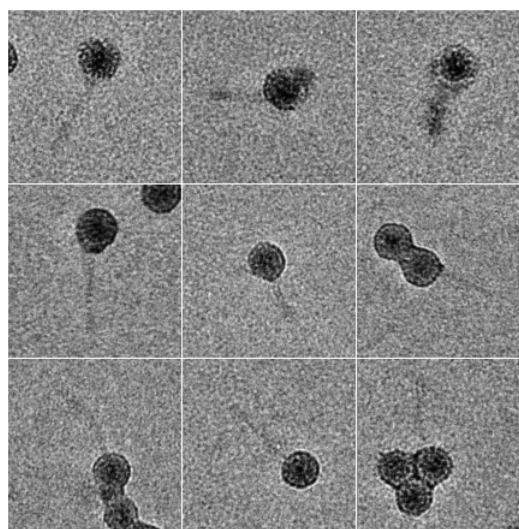

Figure S1. Positive stain TEM images of cherry bomb assembly products that show the ds-RNA-DNA "fuse".
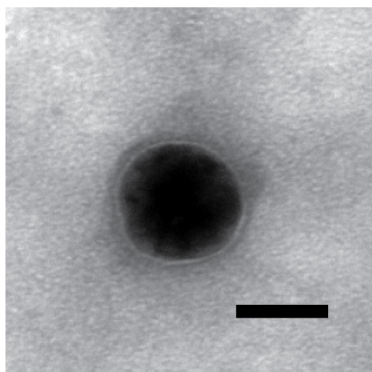
Figure S2. 30-nm AuNP coated with poly-T_{25} imaged by negative-stain TEM. Scale bar shows 25 nm.

Testing for non-specific binding between CCMV VLPs and poly-T_{25}-coated AuNPs

A control co-assembly reaction involving CCMV CP and pure B1 RNA was performed in parallel with the cherry bomb assembly reactions. The assembly products of the control reaction were then mixed with poly-T_{25}-coated AuNPs, equilibrated for 5 min on ice, and imaged by negative-stain TEM (Fig. S3). The same conditions were used to assess the binding of cherry bomb capsids with the poly-T_{25}-coated AuNPs. The control micrographs revealed no evidence of non-specific VLP-AuNP binding.
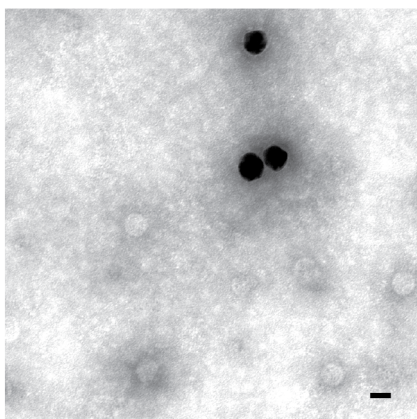

Figure S3. 30-nm AuNPs coated with poly-T_{25} (dark spheres) were incubated with VLPs containing pure B1 RNA (light spheres) and imaged by negative-stain TEM. There is no interaction between VLPs and AuNPs. Scale bar shows 25 nm.

Aggregated assembly of CP around surface-bound RNA

Hybridized RNA-DNA was prepared and equilibrated with 30-nm poly-T_{25}-coated AuNPs at a molar ratio of 10:1 (RNA:AuNP) for 30 min on ice. After hybridization of the RNA to the AuNPs, CP was added at a mass ratio of 10:1 (CP:RNA), equilibrated for 5 min on ice, and imaged by negative-stain EM (Fig. 5B). We used a higher amount of CP (compared to the 6-fold mass ratio used to completely package unbound RNA[3,4]) in case a fraction of the CP was bound by the excess of poly-T_{25} DNA oligos coating the surface of the AuNPs. Indeed, TEM images showing thickened layers of material coating the AuNP surface suggest that CP does bind the poly-T_{25}-coating (Fig. S4). Earlier assembly studies[3] using pure RNA showed that CP:RNA mass ratios higher than 6:1 can result in aggregation. This phenomenon may contribute to the aggregation we see in the AuNP-bound assemblies (Fig. S4).
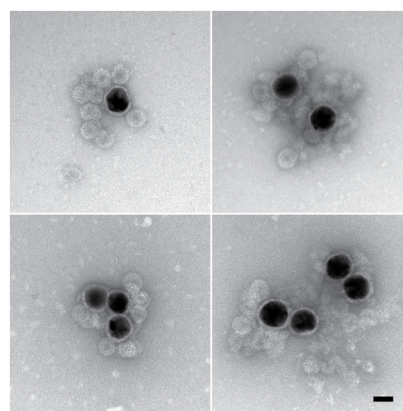

Figure S4. VLP assembly around RNA-DNA bound to the surface of 30-nm AuNPs coated with poly-T_{25} showed significant aggregation. The three types of aggregation seen are (i) an extra layer of material coating each AuNP (thick white halos surrounding electron-dense AuNP found in all images), (ii) extended capsid structures (upper-left image), and (iii) amorphous aggregation (upper-right and lower-right images). Scale bar shows 25 nm.

Transmission Electron microscopy (TEM)

Negative-stain: 6 µL of sample at a concentration of a few nM was deposited on glow-discharged copper grids (400-mesh) that previously had been coated with Parlodion and carbon. After 1 min, the grids were blotted and stained with 6 µL of 2% uranyl acetate for 1 min followed by blotting and storage in a desiccator overnight.

Positive stain: Inevitably, some regions of a negative-stained TEM grid exhibit positive staining. In these regions stain penetrates the sample particles, rather than coating them. We have found that certain structural features are sometimes better resolved

through positive staining – in this case, the RNA-DNA hybrid appendage was more visible in positive-stained regions (Fig. S1).

Native agarose gel electophoresis

10 µL of sample was mixed with 3 µL of glycerol and loaded into a 1% agarose gel in virus electrophoresis buffer (0.1 M sodium acetate, 1 mM EDTA, pH 5.5). The samples were electrophoresed at 4°C at 50 V for 1 h and visualized with a FX Pro Plus Fluorimager/PhosphorImager (Bio-Rad) by exciting the UTP-AF488 of the B1 RNA and 6-FAM of the poly-T$_{15}$, separately, and measuring the emitted fluorescence intensity. The emission intensity of UTP-AF488 (RNA) is shown in red, and that of 6-FAM (poly-T) is shown in green.

REFERENCES

(1) Annamalai, P.; Rao, A. L. N. *Virology* **2005**, *332*, 650.
(2) Garmann, R. F.; Comas-Garcia, M.; Gopal, A.; Knobler, C. M.; Gelbart, W. M. *J. Mol. Biol.* **2014**, *426*, 1050.
(3) Cadena-Nava, R. D.; Comas-Garcia, M.; Garmann, R. F.; Rao, A. L. N.; Knobler, C. M.; Gelbart, W. M. *J. Virol.* **2012**, *86*, 3318.
(4) Garmann, R. F.; Comas-Garcia, M.; Koay, M. S.; Cornelissen, J. J.; Knobler, C. M.; Gelbart, W. M. *J. Virol.* **2014**, *88*, 10472.
(5) Hurst, S. J.; Lytton-Jean, A. K.; Mirkin, C. A. *Anal. Chem.* **2006**, *78*, 8313.